Macromolecules

ARTICLE

pubs.acs.org/Macromolecules

Structural Changes in PEO−PPO−PEO Gels Induced by Methylparaben and Dexamethasone Observed Using Time-Resolved SAXS

Norman A. K. Meznarich,[†] K. Anne Juggernauth,[†,‡] Kiersten M. Batzli,[†] and Brian J. Love*[,†,§,⊥]

[†]Department of Materials Science and Engineering, [‡]Macromolecular Science and Engineering Research Center, [§]Department of Biomedical Engineering, and [⊥]Dental & Biologic Materials (Dental School), University of Michigan, 2300 Hayward Street, Ann Arbor, Michigan 48109, United States

ABSTRACT: Aqueous solutions of polyoxyethylene−polyoxypropylene−polyoxyethylene (PEO−PPO−PEO) triblock copolymers (commercially available as Pluronic surfactants) micellize and structurally arrange into cubic quasicrystalline lattices as their temperature is raised. This structural evolution is seen macroscopically as a gelation, and the presence of these ordered phases can be controlled through both polymer concentration and temperature. The presence of added solutes within the dispersions can also affect the onset and kinetics of structure formation. Here we investigate the structures formed in Pluronic F127 solutions ranging from 20 to 30% with two pharmaceutical additives [methylparaben (MP) and dexamethasone (DX)] using small-angle X-ray scattering (SAXS). We observe both the progressive evolution and breakdown of these structures as the temperature is increased from 0 to 80 °C. Additionally, we conducted time-resolved SAXS measurements to elucidate the kinetics of the structural evolution. On the basis of the evolution of scattering peaks as the samples were being heated, we suggest that added MP changes the nucleation behavior of fcc phases within the sample from a heterogeneous process to a more homogeneous distribution of nucleated species. MP and DX also stabilize the micelle lattices, allowing them to persevere at higher temperatures. We observed the unusual result that the presence of DX caused the primary peaks of the structure factor to be suppressed, while preserving the higher order peaks. The primary peaks reappeared at the highest temperatures tested.

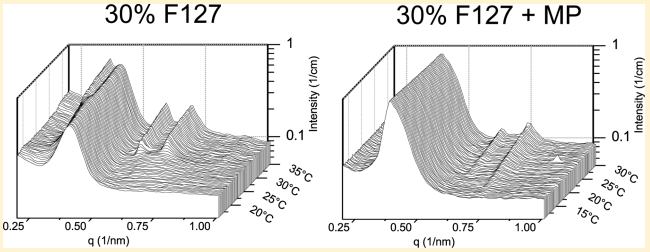

INTRODUCTION

The temperature-dependent micellization and ordering of PEO−PPO−PEO triblock copolymers in aqueous solutions has been the subject of previous review papers.[1,2] Of particular interest is Pluronic F127 (PEO_{99}−PPO_{65}−PEO_{99}), as it has the most pronounced gel forming abilities of the commercially available Pluronic surfactants.[3] As the temperature of these solutions is increased, the decreasing aqueous solubility of the PPO segments causes micelle formation with relatively hydrophobic (PPO) cores and relatively hydrophilic (PEO) shells. It has been suggested by Lam et al.[4] that the micelles grow via Ostwald ripening and by Barba et al.[5] that the volume fraction occupied by the micelles in solution increases with increasing temperature. The micelles experience repulsive interactions and order into quasicrystalline cubic lattices. The typical lattice structures observed for F127 gels are fcc or bcc.[6,7] This lattice structure is believed to give these materials their gel-like properties. The micellization and ordering process is completely reversible as there is no chemical cross-linking of the polymer chains typical of most polymer hydrogels.

This reversible temperature-dependent gelation behavior is of interest to biomedical researchers, owing to the high biocompatibility of F127 and the ability to control the gelation temperature of F127 through concentration.[8−12] These solutions can be injected as a liquid at low temperatures, which then form gels *in situ* as the solution warms to body temperature. The gel formation regulates the release of added pharmaceuticals or agents,[12] providing a more sustained delivery and longer local residence time.

It is known that ternary additives can influence the aqueous F127 micellization and gelation behavior. Methylparaben (MP), for example, lowers the gelation temperature of F127 solutions by as much as 10−15 °C.[13,14] In light of the potential importance of F127 in controlled release, a structural evaluation is merited to understand the structure−property relationship that exists in these pharmaceutical loaded F127 formulations.

Additionally, the gelation kinetics of F127 systems is less well-known. We have investigated the effect of heating rate on the gelation of both F127 and F127 + MP solutions and found that not only does the presence of MP lower the gelation temperature, it also accelerates the gel transition.[14] These measurements, however, only indirectly infer the structure of these solutions as a function of temperature, and a more direct evaluation of structural evolution is needed to better understand the transition from the disordered to the ordered state.

SAXS and SANS scattering have been used extensively to study the structure and organization of micellar systems.[6,15−17]

Received: July 5, 2011
Revised: August 17, 2011
Published: September 07, 2011

dx.doi.org/10.1021/ma2015358 | *Macromolecules* 2011, 44, 7792–7798

These techniques allow insight into both the structures within the micelles and also the lattice structures into which they arrange. Previously, Sharma et al.[18] used SANS to investigate the effects of added pharmaceuticals on the nanoscale structure of F127 micelles. These results, however, focused on the properties and formation of the micelles themselves, and changes to the micelle lattice structures were not considered. Here we use SAXS to investigate the crystalline structure of F127 solutions as they are heated through their gelation temperatures. Our aim is to identify changes in quasicrystalline lattice formation as an effect of added pharmaceuticals. We observe structural changes associated with the presence of MP and DX on F127 and examine the different kinetics of gel formation with varying composition. This work leads to a greater understanding of the interactions that added pharmaceuticals have with F127 micelles and the roles they play in modifying the structural interactions between micelles.

METHODS

Solution Preparation. Pluronic F127 was obtained from Sigma-Aldrich (St. Louis, MO) and used as received. Solutions ranging from 20 to 30% w/w were prepared using the cold method of Schmolka[3] by dissolving weighed amounts of F127 into distilled water, which were then left to solubilize quiescently at 4 °C. For the high concentration solutions, repeated cool/mix cycles were needed to fully solubilize the polymer.

Methylparaben (MP) was also obtained from Sigma-Aldrich (St. Louis, MO) and used at a concentration of 1% w/v. A stock solution of 10% F127 and 1% MP was prepared, and weighed amounts of F127 were added to aliquots of the stock to obtain solutions of increasing F127 concentration. A similar method was used to prepare solutions containing dexamethasone (DX), also from Sigma-Aldrich. As the solubility of DX is low in aqueous solutions, it was added to saturation rather than to a predefined concentration. We estimate the final concentration of added DX to be less than 0.5% w/v. The structures of the added pharmaceuticals are shown in Figure 1.

For clarity, the compositions tested in this paper will be hereafter referred to by the following naming convention. Two digits will represent the F127 concentration, followed by two letters for the composition. PL for neat F127, MP for solutions containing added methylparaben, and DX for solutions saturated with dexamethasone. For example, a 25MP solution represents 25% w/v F127 with 1% w/v MP.

Small-Angle X-ray Scattering. SAXS experiments were conducted at Argonne National Laboratory (Argonne, IL) at the Advanced Photon Source (APS) on beamline 5-ID, and at Brookhaven National Laboratory (Upton, NY) at the National Synchrotron Light Source (NSLS) on beamline X10A. Thermal control was provided by a Linkham (Guildford, UK) THMS600 heating stage.

Two types of scattering experiments were conducted. Static heating tests were used to probe the structure at a series of discrete temperatures between 0 and 80 °C. The sample was loaded into the heating stage and subjected to 2 min equilibration time at 0 °C to ensure that the sample temperature was uniform and steady. Scattering data were collected followed by a 10 °C rise in temperature and subsequent 2 min equilibration period. This process was repeated up to a final temperature of 80 °C. During the heating and equilibration phases, the X-ray shutters were closed to avoid unnecessary exposure to the beam.

Time-resolved SAXS studies allowed the investigation of the kinetics of structural evolution. For these tests, the sample was loaded into the heating stage and equilibrated at the starting temperature. After equilibration, the sample was heated at a rate of 1 °C/min to the final temperature. Continuous data acquisition at ~30 s intervals was carried out for the duration of the heating. The starting and final temperatures were chosen to be roughly 5−10 °C below and above the gelation temperature of the sample, respectively. This was done so the entirety of the ordering event could be captured during the experiment and to allow any temperature-lagging processes to complete before the end of the data collection.

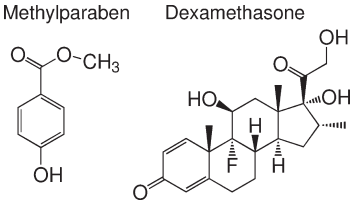

Figure 1. Structure of the two added pharmaceuticals, methylparaben (MP) and dexamethasone (DX).

Table 1. Summary of Expected Peaks and Relative Peak Positions for the bcc and fcc Crystal Systems

crystal	q_0	q_1	q_2	q_3	q_4
bcc	(110)	(200)	(211)	(220)	(310)
position	q_0	$2^{1/2}q_0$	$3^{1/2}q_0$	$2q_0$	$5^{1/2}q_0$
fcc	(111)	(200)	(220)	(311)	(222)
position	q_0	$(4/3)^{1/2}q_0$	$(8/3)^{1/2}q_0$	$(11/3)^{1/2}q_0$	$2q_0$

Data Collection and Analysis. 2D SAXS data were collected using a CCD detector at each beamline. The data were integrated around the azimuthal axis to generate 1D plots of the measured intensity as a function of the scattering vector q. By combining Bragg's law (eq 1) and the definition of the reciprocal space scattering vector (eq 2), one can relate q to the scattering angle (eq 3), where 2θ is the scattering angle, d is the real space lattice vector, and λ is the X-ray wavelength.

$$\lambda = 2d \sin\theta \tag{1}$$

$$q = \frac{2\pi}{d} \tag{2}$$

$$q = \frac{4\pi}{\lambda} \sin\theta \tag{3}$$

Peak positions in the generated $I(q)$ plots were quantified using OriginLab's peak analyzer function. These peaks were then compared to the expected reflections for the various known crystal structures in order to identify the structures present in the solution. Table 1 presents a brief summary of the first five expected peaks and their positions relative to the fundamental scattering peak for the fcc and bcc crystal systems.

RESULTS

Figure 2 compares the presence of ordered phases by sample composition. Moving down the columns shows the effect of decreasing F127 concentration. Moving across the rows shows the effect of added MP and DX. The presence of MP lowers the temperature where ordering occurs relative to neat F127 samples. For example, an ordered phase is first seen in the 20 °C measurement for 30MP (Figure 2b) sample as compared to 30 °C for the 30PL (Figure 2a) sample. This is consistent with our previously reported[14] work indicating a lowering of the gelation temperature with added MP. Similar behavior is observed for added DX.

For lower F127 concentrations, similar trends were observed to those seen with 30% solutions. However, breakdown of the

dx.doi.org/10.1021/ma2015358 |Macromolecules 2011, 44, 7792–7798

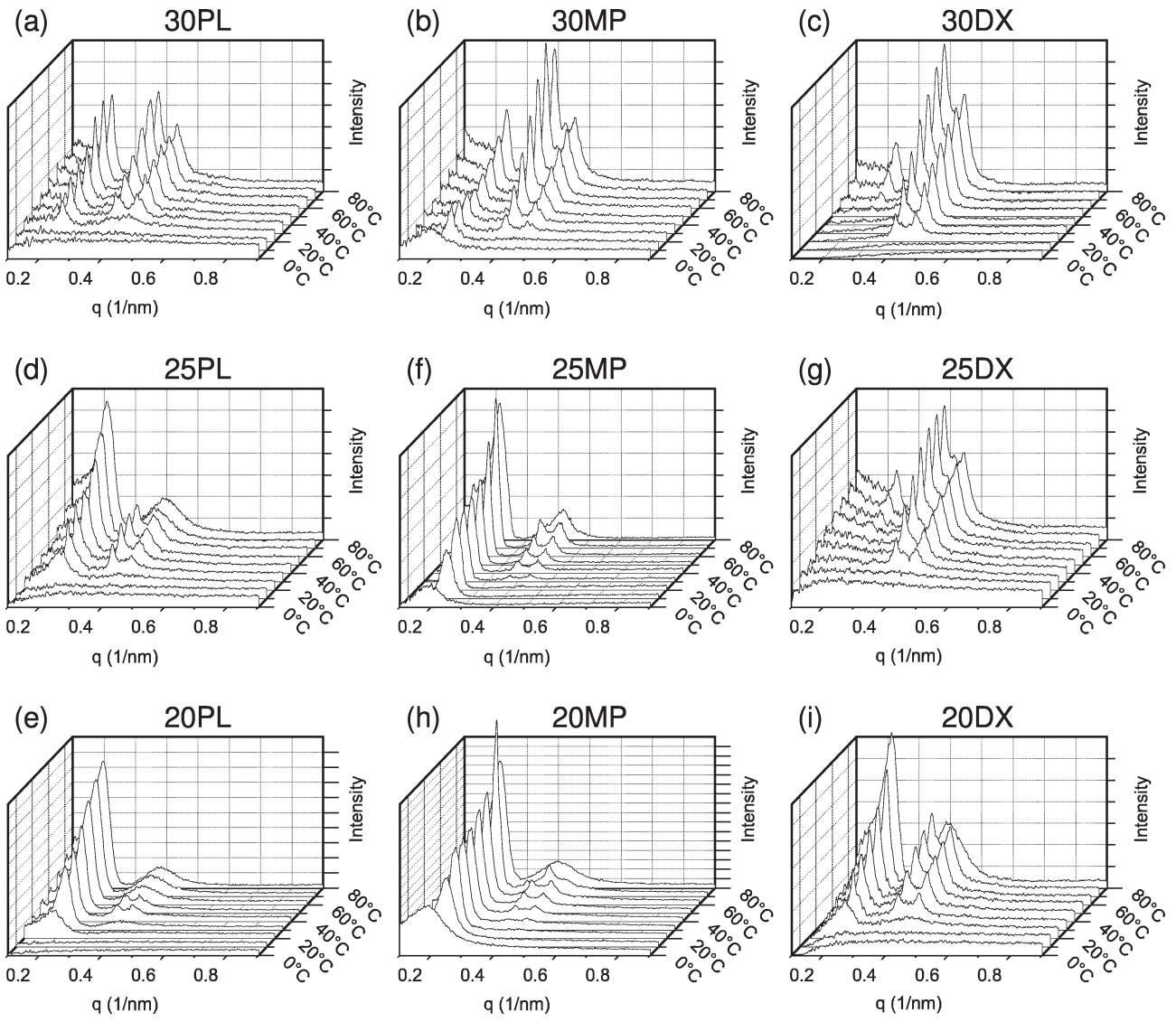

Figure 2. Comparison of the presence of ordered phases as a function of F127 concentration (columns) and pharmaceutical additive (rows) using representative data sets from each condition. The vertical intensity scale is a raw count from the detector, with each tick mark representing 500 counts.

ordered phases is evident at high temperatures. Figures 2d and 2e show the phases present in 25PL and 25MP, respectively. At 70 °C and above, the 25PL sample does not show any ordered phase, instead showing a broad amorphous peak. The 25MP sample, however, preserves the ordered phase at 70 °C, indicating an MP-induced stabilization of the quasicrystalline lattice in F127 gels. DX is even more effective at preserving ordered phases even at the maximum temperature of 80 °C as evidenced by the presence of sharp peaks in Figure 2g for 25DX. A similar high-temperature stabilization of the structure is seen for 20% F127 as well.

Tables 2 and 3 show the identified peak positions for each sample in Figure 2 and the associated crystal structure identified from peaks present at 40 and 70 °C, respectively. Most of the identified phases are fcc. Although the fcc (200) peak at $(4/3)^{1/2}q_0$ is not seen, the (220) and (311) peaks (at $(8/3)^{1/2}q_0$ and $(11/3)^{1/2}q_0$, respectively) are clearly identifiable in all cases. The lack of a distinct (200) peak could be due to fcc twinning defects in the quasicrystalline lattice, where portions of the structure deviate from the ABCABC fcc structure to the ABABAB or ACACAC hcp structure. This defect has been known to suppress individual Bragg peaks.[19−21] It can also be seen from the plots in Figure 2 and the corresponding data in Tables 2 and 3 that, at

Table 2. Fundamental (q_0) and Higher Order (q_n) Peaks (in Units of nm^{-1}) and Identified Phase at 40 °C

sample	q_0	q_1	q_2	phase
30PL	0.2233	0.3696	0.4346	fcc
30MP	0.2364	0.3866	0.4547	fcc
30DX	*a*	0.3796	0.4457	likely fcc
25PL	0.2135	0.3569	0.4150	fcc
25MP	0.2253	0.3726	0.4367	fcc
25DX	*a*	0.3836	0.4467	likely fcc
20PL	0.2063	0.3435	0.3936	fcc
20MP	0.2233	0.3655	0.4276	fcc
20DX	0.2173	0.3635	0.4296	likely fcc

[a] No fundamental peak was present at this temperature but visible at higher temperatures.

dx.doi.org/10.1021/ma2015358 |*Macromolecules* 2011, 44, 7792–7798

Table 3. Fundamental (q_0) and Higher Order (q_n) Peaks (in Units of nm^{-1}) and Identified Phase at 70 °C

sample	q_0	q_1	q_2	q_3	q_4	phase
30PL	0.2233	0.3726[a]	0.4346[a]			fcc
30MP	0.2344	0.3856[a]	0.4216[b]	0.4527[a]		fcc + bcc
30DX	0.2263	0.3806[a]	0.4457[a]			fcc
25PL	0.2175	0.3829				none
25MP	0.2253	0.3685[a]	0.4306[a]			fcc
25DX	0.2273	0.3816[a]	0.4447[a]			fcc
20PL	0.2003	0.3756				none
20MP	0.2273	0.3245[b]	0.3946[b]	0.4417[b]		bcc
20DX	0.2223	0.3245[b]	0.3655[a]	0.3976[b]	0.4256[a]	fcc + bcc

[a] fcc peaks. [b] bcc peaks, based on their ratio to the fundamental peak.

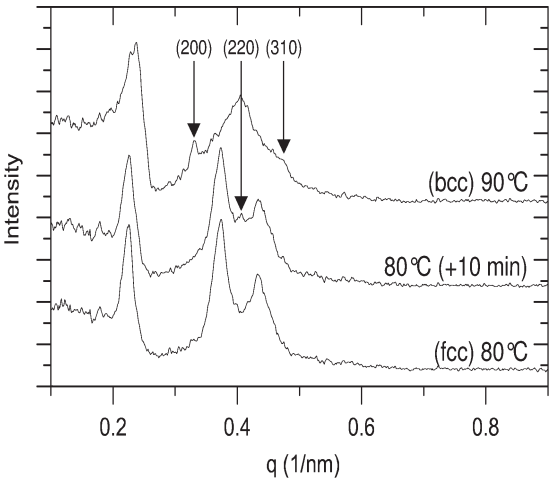

Figure 3. Appearance and transition from the fcc phase (80 °C) to the bcc phase (90 °C) for a 30PL solution at high temperatures. The graph shows the sample at 80 °C (bottom), 80 °C after an additional 10 min of incubation (middle), and at 90 °C (top). The center arrow highlights the emergence of a bcc (220) peak at 80 °C after incubation, and the outer two arrows show the bcc (200) and (310) peaks appearing upon subsequent heating to 90 °C.

high temperatures, there is sometimes a slight emergence of bcc phases (peaks at $2^{1/2}q_0$, $3^{1/2}q_0$, $2q_0$) alongside the usual fcc scattering rings. Figure 2h shows clearly that for 20MP a nearly complete transition to the bcc phase was observed at 70 °C.

For some samples, bcc contributions to the phase structure were not initially observed upon reaching the highest temperature; however, after a period of incubation, bcc peaks began to form. Figure 3 shows SAXS profiles of a 30PL sample at high temperature. Upon initially reaching 80 °C, the sample does not exhibit peaks associated with the presence of a bcc phase. After incubating for 10 min at 80 °C, however, the (200) bcc peak becomes visible (center arrow). When the temperature was raised to 90 °C, the bcc phase becomes dominant, with the (200) and (310) peaks becoming visible (outer arrows). This observation is not to be confused with peak broadening and breakdown of structure at high temperatures (which can be seen in lower concentration samples as illustrated in Figure 2) as the intensity of these new peaks is high compared to the amorphous scattering peaks, and the three distinct peaks can be correlated with the calculated bcc lattice structure (Table 1). Additionally,

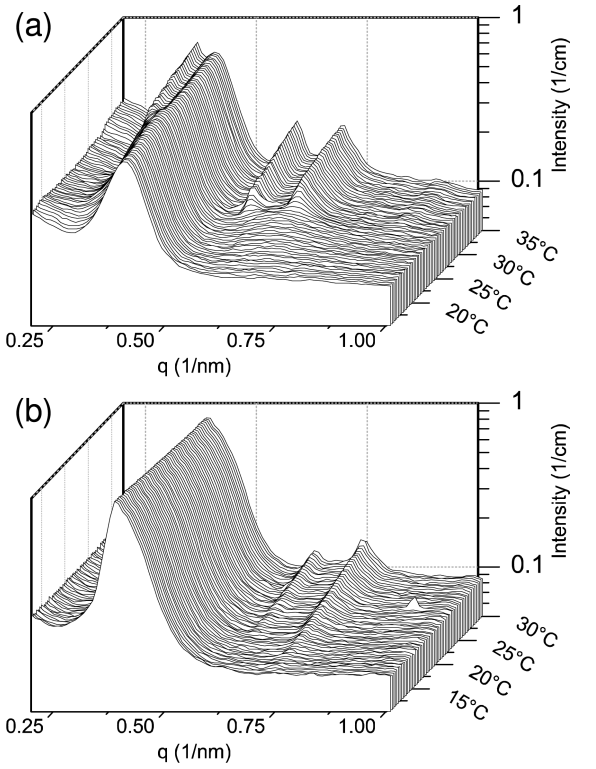

Figure 4. Time-resolved SAXS of 30PL (a) and 30MP (b) samples heated at a rate of 1 °C/min through their transition temperatures: 15−35 °C for 30PL and 10−30 °C for 30MP. The appearance of the ordered state occurs more rapidly in 30PL vs 30MP.

further incubation at 90 °C resulted in the peaks still being visible with no evidence of breakdown, suggesting that the bcc phase is stable.

We found that the onset of the ordered phase differed greatly between 30PL and 30MP samples. Figure 4 shows time-resolved SAXS plots of 30PL and 30MP samples (parts a and b, respectively) as they were heated through their gelation temperatures. The emergence of fcc peaks in 30PL is rapid and occurs over the span of a few frames (∼1−2 min elapsed time), whereas the fcc quasicrystalline phase in 30MP gradually increases in prominence throughout the duration of the experiment. It should be noted that the positions of the peaks in Figure 4 differ from the reported 30PL and 30MP peak positions in Tables 2 and 3. The reason for this is that the data shown in Figure 4 were collected at the APS, where a different beam wavelength λ was used, causing a shift in the q positions of the peaks. However, based on the relative positions of the higher order peaks to the fundamental peak, the structure represented is still fcc.

Finally, another key difference observed from adding MP is the appearance of the scattering rings. Figure 5 shows the scattering rings for F127 samples (particularly those of high concentration, 25% or greater) have a nonuniform or "speckled" appearance, with bright spots of intense scattering randomly arranged around a lower intensity halo. Wanka et al.[1] also observed this behavior in 30% w/v F127 gels using SANS, which he similarly described as "high intensity spikes superimposed on [a] smooth correlation ring". We attribute this observation to the presence of discrete domains containing organized micelles, somewhat akin to coarse granular polycrystalline materials. In

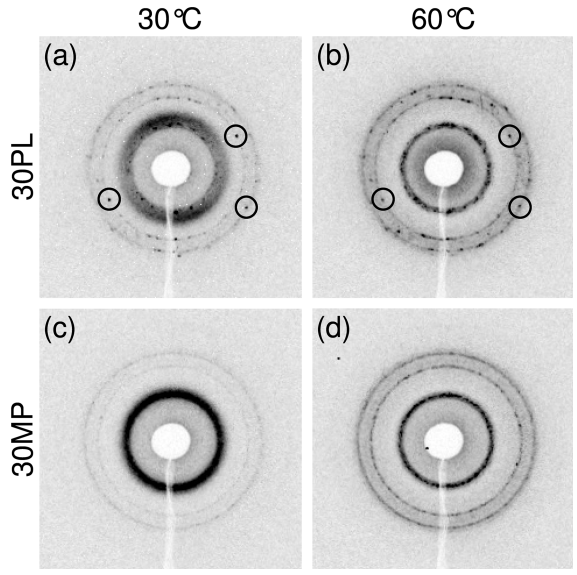

Figure 5. Comparison between a 30PL (a, b) and 30MP (c, d) sample at 30 and 60 °C. The scattering rings in the 30PL sample have a distinct "speckled" appearance, whereas the 30MP sample has smoother, more uniform rings. Spots within the 30PL sample do not move as the temperature is increased (circled examples); new spots appear as additional ordered domains are nucleated.

contrast, the 30MP samples exhibit a smoother ring appearance, indicating a scattering behavior more similar to that of a powder, where the domains within the scattering volume cover all possible orientation angles.

■ DISCUSSION

We observed that MP gels exhibited a more gradual transition from the disordered state to the fcc ordered state as compared to neat F127 gels, as seen using time-resolved SAXS (Figure 4). The 30PL (Figure 4a) sample shows a broad amorphous scattering peak (located at $q = 0.406\ \mathrm{nm}^{-1}$) at the starting temperature, and at around 25 °C, three distinct fcc peaks (located at q = 0.367, 0.592, and $0.700\ \mathrm{nm}^{-1}$) appear. The amorphous scattering peak, however, is still visible after the fcc phase appears. Figures 5a and 5b also illustrate that as the temperature rises and additional domains of fcc phase are created, the scattering intensity of the amorphous halo decreases as an increasing number of "free" micelles are incorporated into ordered domains. Additionally, the spots of intense coherent scattering remain stationary as the sample is heated (circled examples in Figure 5), indicating that ordered domains, once formed, remain stable. This suggests that the fcc phase forms via a nucleation and growth mechanism, where pockets of fcc phase are emerging from a larger expanse of amorphous or uncorrelated micelles. As the temperature is further increased, micelles are drawn from the amorphous regions and arranged into the ordered regions, or new sites of fcc phase are created.

Comparing Figures 4a and 4b, it is possible that the nucleation behavior is different when F127 solutions contain MP as a ternary constituent. The appearance of the fcc peaks is a gradual process, occurring over the entire heating period. Figures 5c and 5d also demonstrate this; as the intense central ring becomes sharper with increasing temperature, indicating a more refined fcc structure being present. In addition, the average intensity around the azimuthal axis is more uniform; i.e., the scattering rings are smoother in appearance. These observations suggest that the nucleation of the fcc phase within the MP samples has a more homogeneous distribution as compared to the PL samples, where a relatively fewer number of nuclei are active but grow more rapidly.

It can also be seen in Tables 2 and 3 that added MP and DX had a small effect on the position of the scattering peaks. For solutions with added MP or DX, the peaks were shifted to the right (positive increase) by approximately $0.01-0.02\ \mathrm{nm}^{-1}$ on the q scale. Adding MP reduced the calculated d_{111} spacing for 30% mixtures from 48.74 to 46.42 nm, indicating a "tighter" lattice. Based on our prior work using DLS to determine micelle size,[14] the presence of MP seems to increase the micelle monodispersity, which may in turn lead to tighter packing with fewer defects in the lattice, thus producing the small observed shift in the lattice parameter. Further studies are needed to better characterize the size of F127 micelles with added MP and DX. The additives may play a role in facilitating transitions between regions within the micelle (for example, reducing the interfacial energy of the core−shell boundary) or perhaps acting as a plasticizer within the micelle core and chaperoning polymer chain transfer between micelles.

Previously, Nagarajan[22,23] measured the solubility of hydrophobic "guest" molecules (mainly hydrocarbon chains) in PEO−PPO−PEO triblock micelles. The presence of amphiphilic molecules aids in the solubilization of these hydrophobic molecules. It is likely that the "guest" molecules localize to the micelle core, where they either uniformly disperse throughout the core or form a separate domain at the center of the core (resulting in an inner core of "guest" molecules and an outer core of hydrophobic polymer blocks). Similar studies have been carried out to measure the localization or interaction of other ternary additives with PEO−PPO−PEO micelles.[24−26] On the basis of this prior work, and the molecular structures of MP and DX (Figure 1), we believe that the added MP and DX are also localized to the micelle cores. Considering the high hydrophobicity of DX (with an *n*-octanol/water partition coefficient of ~1.95[27]), it may even be energetically favorable for DX molecules to phase separate within the micelle cores themselves, producing an inner core of DX and an outer core of PPO, surrounded by a PEO shell.

Regarding our previous finding that added MP suppresses the micellization endotherm of F127 solutions,[14] these SAXS measurements clearly demonstrate that ordered periodic structures still exist in MP containing solutions. This observation is strong evidence that although no micellization endotherm was observed via DSC in our previous work, these solutions still undergo the typical micellization and ordering steps seen in neat F127 solutions.

We observed that, while the structure of these gels is primarily fcc, some bcc component is in certain cases detected at high temperatures. Mortensen et al.[6] also showed an fcc to bcc transition with increasing temperature in F127 samples purified of diblock impurities. Similar fcc to bcc transitions have also been observed in polystyrene−polyisoprene and poly(oxyethylene)−poly(oxybutylene) diblock polymer systems.[28,29] One explanation for this behavior is a change in the stiffness or size of the micellar corona as the temperature changes. At higher temperatures, a softening (or thicker) corona tends to favor bcc packing, whereas at lower temperatures, a stiffer (or thinner) corona tends to favor an fcc arrangement.[6] This fcc to bcc phase transition was also predicted in calculations made by

Semenov.[30] The appearance of the bcc phases also has a kinetic component, as we were able to observe bcc peaks at 80 °C after extended incubation, whereas no bcc peaks were found when the sample was initially raised to 80 °C (Figure 3).

The stabilizing effect of MP and DX on the ordered phases was evident at all concentrations tested. Initiation of ordering is observed in the solutions containing ternary additives at lower temperatures when compared to the neat F127 solutions. This is strong evidence to suggest enhanced micelle ordering, which leads to the corresponding drop in gel temperature previously observed by other methods.[13,14] Yang et al.[31] studied the effect of polydispersity on the stability of hard-sphere colloidal crystals and found that increasing polydispersity decreases the stability of fcc crystals. It is possible that the extended range of temperatures in which fcc phases are seen in MP and DX containing solutions is due to the decreased polydispersity we have observed in prior experiments,[14] which stabilize the ordered phases in solution.

Regarding the effect of added pharmaceuticals on the presence of bcc phases, MP or DX did not have any significant or systematic influence on the emergence of the bcc phase we observed. We identified bcc components at high temperatures in PL, MP, and DX samples tested. Additionally, we observed at least one instance of a relatively complete fcc to bcc transition in both neat and MP samples (Figures 3 and 2h, respectively).

The missing fundamental peak in the DX samples was unexpected. A search of previous literature resulted in only a single reference to a similar phenomenon. Olsen et al.[32] reported suppression in the fundamental peak intensity while studying thin films of poly(alkoxyphenylenevinylene-*b*-isoprene) rod−coil copolymers arranged into lamellar structures. They were unable to explain the origin of this effect. Considering the behavior of ternary additives in PEO−PPO−PEO micelles discussed earlier in this section, one possible explanation for our observations is that the scattering behavior upon adding DX adopts a core−shell form factor. In the case of the PL and MP samples, the scattering behavior only has a contribution from the PPO micelle cores, but in the case of DX, scattering from both an inner DX core and PPO outer core is possible. This is because the scattering contrast between PEO and water is low, and the highly solvated nature of the PEO block further serves to reduce scattering contrast from the micelle shell.[24] In the case of DX, it is conceivable that scattering occurs from both a DX inner core and a PPO outer core. The scattering interactions between this inner core/outer core structure (which can be thought of as a core and a shell) might suppress SAXS as seen in the DX samples.

At higher temperatures, the fundamental scattering peaks in the DX samples emerge. The solubility of the PPO blocks decreases with increasing temperature, effectively increasing the hydrophobicity at high temperatures.[33] Therefore, if the PPO blocks became sufficiently hydrophobic, intermixing of the PPO blocks with DX inner core may occur and produce a homogeneous core, removing the core−shell scattering interactions and allowing the primary fcc peak to reappear. It is also interesting to note that the 20DX sample did not exhibit this fundamental peak suppression, indicating some concentration dependence of this phenomenon.

Although we focused our efforts on measuring F127 concentrations of 20% and above, some experiments were conducted at F127 concentrations of 15% and below. At these concentrations, no fcc structure or other distinct scattering rings were observed for neat F127. These solutions still micellize and form gels;[14] however, it is likely that the volume fraction of the solution occupied by the micelles is insufficient to form quasicrystalline structures in solution.

CONCLUSION

SAXS analysis of F127 solutions containing MP and DX has revealed several key changes in their phase behavior in the presence of added pharmaceuticals. In general, we observed rather marked changes in scattering behavior, especially considering the low concentrations of added solutes in the tested solutions. The presence of MP and DX facilitates or enhances the structural ordering, allowing ordered phases to emerge at lower temperatures and remain at higher temperatures as compared to the neat F127 solutions. We have found evidence to suggest that the presence of pharmaceuticals affects the mechanism by which the ordered phases evolve. This is can be seen in Figure 2 as well as the distinctive appearance of the scattering rings in Figure 5.

In addition to stabilizing the presence of these structures, addition of MP and DX reduces the lattice plane spacing by a small amount, evidenced by a slight shift in the peak positions to higher q values.

Finally, DX has produced a unique scattering behavior compared with MP or PL samples in that the fundamental scattering peak is suppressed for much of the tested temperature range. This observation suggests that the interactions between DX and MP with F127 micelles are different and that further investigation in this area is needed in order to explain the mechanism behind this behavior.

These experiments show how using time-resolved small-angle X-ray scattering coupled with a dynamic heating protocol, structural changes in amphiliphilic copolymer solutions can be characterized when formulated with ternary additives. Specifically, we have shown here that the evolution of the fcc phase in PEO−PPO−PEO solutions follows a nucleation and growth mechanism. We have also observed that adding MP as a ternary constituent alters the evolution mechanism from a heterogeneous to a homogeneous nucleation. Understanding where therapeutic molecules as ternary additives are partitioned within micelles and how they influence the evolving structure is important to optimize controlled release systems utilizing amphiphilic copolymers as a delivery platform.

AUTHOR INFORMATION

Corresponding Author
*E-mail: bjlove@umich.edu.

ACKNOWLEDGMENT

Portions of this work were performed at the DuPont−Northwestern−Dow Collaborative Access Team (DND-CAT) located at Sector 5 of the Advanced Photon Source (APS). DND-CAT is supported by E.I. DuPont de Nemours & Co., The Dow Chemical Company, and Northwestern University. Use of the APS, an Office of Science User Facility operated for the U.S. Department of Energy (DOE) Office of Science by Argonne National Laboratory, was supported by the U.S. DOE under Contract DE-AC02-06CH11357. Use of the National Synchrotron Light Source, Brookhaven National Laboratory, was supported by the U.S. Department of Energy, Office of Science, Office of Basic Energy Sciences, under Contract DE-AC02-98CH10886. We thank the Department of Education's Graduate

Assistance in Areas of National Need (GAANN) fellowship program for supporting Norman during portions of this work. We also gratefully acknowledge Steve Weigand for his assistance at the APS Sector 5 beamline, Steve Bennett for his assistance at the NSLS X10A beamline, Amy Gros and Marlee Green for their assistance in collecting SAXS data, and Charles M. Shaw for insightful discussions.

REFERENCES

(1) Wanka, G.; Hoffmann, H.; Ulbricht, W. *Macromolecules* **1994**, *27*, 4145–4159.
(2) Alexandridis, P.; Hatton, T. A. *Colloids Surf., A* **1995**, *96*, 1–46.
(3) Schmolka, I. R. *J. Biomed. Mater. Res.* **1972**, *6*, 571–582.
(4) Lam, Y.; Goldbeck-Wood, G. *Polymer* **2003**, *44*, 3593–3605.
(5) Barba, A. A.; d'Amore, M.; Grassi, M.; Chirico, S.; Lamberti, G.; Titomanlio, G. *J. Appl. Polym. Sci.* **2009**, *114*, 688–695.
(6) Mortensen, K.; Batsberg, W.; Hvidt, S. *Macromolecules* **2008**, *41*, 1720–1727.
(7) Jiang, J.; Burger, C.; Li, C.; Li, J.; Lin, M. Y.; Colby, R. H.; Rafailovich, M. H.; Sokolov, J. C. *Macromolecules* **2007**, *40*, 4016–4022.
(8) Nalbandian, R. M.; Henry, R. L.; Balko, K. W.; Adams, D. V.; Neuman, N. R. *J. Biomed. Mater. Res.* **1987**, *21*, 1135–1148.
(9) Hsu, S.-H.; Leu, Y.-L.; Hu, J.-W.; Fang, J.-Y. *Chem. Pharm. Bull.* **2009**, *57*, 453–458.
(10) Kabanov, A.; Zhu, J.; Alakhov, V. Y. *Adv. Genet.* **2005**, *53*, 231–261.
(11) Ohta, S.; Nitta, N.; Takahashi, M.; Sonoda, A.; Tanaka, T.; Yamasaki, M.; Furukawa, A.; Takazakura, R.; Murata, K.; Sakamoto, T.; Kushibiki, T.; Tabata, Y. *J. Vasc. Interv. Radiol.* **2006**, *17*, 533–539.
(12) Escobar-Chavez, J. J.; Lopez-Cervantes, M.; Naik, A.; Kalia, Y. N.; Quintanar-Guerrero, D.; Ganem-Quintanar, A. *J. Pharm. Pharm. Sci.* **2006**, *9*, 339–358.
(13) Sharma, P. K.; Reilly, M. J.; Bhatia, S. K.; Sakhitab, N.; Archambault, J. D.; Bhatia, S. R. *Colloids Surf., B* **2008**, *63*, 229–235.
(14) Meznarich, N. A. K.; Love, B. J. *Macromolecules* **2011**, *44*, 3548–3555.
(15) Wolff, M.; Magerl, A.; Zabel, H. *Thin Solid Films* **2007**, *515*, 5724–5727.
(16) Mortensen, K.; Pedersen, J. *Macromolecules* **1993**, *26*, 805–812.
(17) Prudhomme, R.; Wu, G.; Schneider, D. *Langmuir* **1996**, *12*, 4651–4659.
(18) Sharma, P. K.; Reilly, M. J.; Jones, D. N.; Robinson, P. M.; Bhatia, S. R. *Colloids Surf., B* **2008**, *61*, 53–60.
(19) Loose, W.; Ackerson, B. J. *J. Chem. Phys.* **1994**, *101*, 7211–7220.
(20) Castelletto, V.; Hamley, I.; Holmqvist, P.; Rekatas, C.; Booth, C.; Grossmann, J. *Colloid Polym. Sci.* **2001**, *279*, 621–628.
(21) McConnell, G. A.; Lin, M. Y.; Gast, A. P. *Macromolecules* **1995**, *28*, 6754–6764.
(22) Nagarajan, R. *Colloids Surf., B* **1999**, *16*, 55–72.
(23) Nagarajan, R. *Polym. Adv. Technol.* **2001**, *12*, 23–43.
(24) Ruthstein, S.; Raitsimring, A. M.; Bitton, R.; Frydman, V.; Godt, A.; Goldfarb, D. *Phys. Chem. Chem. Phys.* **2009**, *11*, 148–160.
(25) Steinbeck, C.; Hedin, N.; Chmelka, B. *Langmuir* **2004**, *20*, 10399–10412.
(26) Jia, L.; Guo, C.; Yang, L.; Xiang, J.; Tang, Y.; Liu, H. *J. Phys. Chem. B* **2011**, *115*, 2228–2233.
(27) Caron, J.; Shroot, B. *J. Pharm. Sci.* **1984**, *73*, 1703–1706.
(28) Lodge, T.; Bang, J.; Park, M.; Char, K. *Phys. Rev. Lett.* **2004**, 92.
(29) Hamley, I.; Daniel, C.; Mingvanish, W.; Mai, S.; Booth, C.; Messe, L.; Ryan, A. *Langmuir* **2000**, *16*, 2508–2514.
(30) Semenov, A. *Macromolecules* **1989**, *22*, 2849–2851.
(31) Yang, M.; Ma, H. *J. Chem. Phys.* **2008**, *128*, 134510.
(32) Olsen, B. D.; Li, X.; Wang, J.; Segalman, R. A. *Soft Matter* **2009**.
(33) Alexandridis, P.; Nivaggioli, T.; Hatton, T. A. *Langmuir* **1995**, *11*, 1468–1476.